Part I.

Introduction to the Background Theory and Open Scientific Issues

4. The Base of Our Knowledge – The Moon, Earth and Venus

The Moon, our closest neighbour, is the best studied extraterrestrial object in our solar system. Moreover, the target of the first space missions culminating in manned landing and sample–return during the American Apollo and Russian Luna Programs (1969–1976). Therefore, the Moon is the only planetary body, apart from Earth, where we can relate rock samples as well as their composition and age, more or less confidently to specific geomorphologic units. Furthermore, based on isotope ratios and chemical composition, the differentiation of the Moon ended long ago, and based on its small size the Moon is considered to be no longer geologically active. The two dominant geological processes that have sculpted the lunar surface are impact cratering and mare volcanism. Volcanism as a surface shaping process has ended but impact cratering is still ongoing and is a process relevant to this thesis. The Moon has preserved much of its surficial magmatic and cratering record for most of its life span. Lunar surface interpretation allows us to look back into the early phase of planetary evolution, while on Earth, plate tectonics and resurfacing processes driven by large–scale mantle convection, change the visible surface and have erased most of its impact record. The current impact crater distribution on Earth (Fig. 4.1) is basically controlled as on any other extraterrestrial solid–surface body by its surface or crustal age.

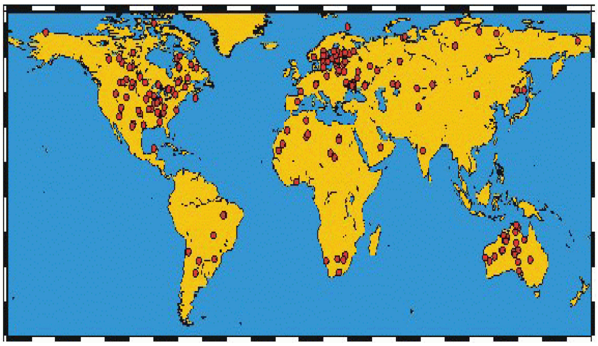

Figure 4.1.: Impact crater Distribution on Earth: Due to plate tectonics and erosional processes the impact crater population on Earth has been strongly modified. Especially oceanic crust is widely unaffected by craters due to its young age (less than 175 Ma). (Source: Earth Impact Database at the PASSC, University of New Brunswick, Canada)

The Earth

The densely cratered units are correlated with the cratons (based on crater counts, their mean age is $\sim$ 400 Ma, (Neukum, 1983), while the crystallization ages of the rock could vary). The lack of craters in the oceanic crust is due to two reasons: (1) In general, oceanic crust is very young (on average 62 Ma; maximum age is $\sim$ 175 Ma) and almost no craters are expected (Koulouris *et al.*, 1999). (2) Small impactors (less than $1-2$ km in diameter) do not affect the ocean floor because the motion of such projectiles is already decelerated when they reach a depth of about 1.5 km (Shuvalov, 2003) while the average depth of the ocean is about 5 km. Only a single impact event in deep water is known and there no crater is present: Eltanin in the Bellingshausen Sea (Gersonde *et al.*, 1997). Crater records on land of the smaller–size range ($<$ 5 km) can be either erased by geological processes, e. g. erosion, or later exhumed after being buried under a protecting cover. Hence their frequency might not represent the real surface age (e.g. in Fennoscandia). Both processes have to be considered when crater size–frequency distributions are measured on planetary surfaces which are geologically more active than the Moon.

Venus

An additional factor on terrestrial crater size–frequency distributions is the shielding effect of the atmosphere, which on Venus is even stronger than on Earth (Ivanov *et al.*, 1992; McKinnon *et al.*, 1997). On Venus projectiles producing craters of diameters less than approximately 1 km are disrupted and possibly hit the surface as a swarm of fragments creating impact crater clusters, if they reach the surface at all. On the other hand, the recognition of craters on Earth's surface is highly biased by the accessibility of the area and the research activity within a specific region.

The Earth can be used as an analogue, but has its clearly limitations when exploring the past, although the well-dated rock record is of tremendous value. Therefore, the Moon has become, based on its cratering record, a time–stratigraphic calibration reference for the Earth–Moon system and the entire inner Solar System. A combination of interpreting ground–based and orbiter–based multispectral imagery and in–situ data promote the Moon (apart from the Earth) to be a valuable test case and calibrator for many methods based on remote sensing data.

4.1. Geologic Evolution of the Moon

The formation and evolution of the Moon is part of the evolution of the planetary system. Even in modern times, hypotheses of the origin of the Moon include capture from an independent solar orbit, rapid co–accretion or fission from the Earth. A variant of the fission hypothesis is that the Moon accreted rapidly from ejecta of a massive (proto–mars sized) impact on the Earth after its core had formed (Hartmann and Davis, 1975; Cameron and Ward, 1976; Cameron, 1986). These later alternatives are based on the commonly accepted idea that the Moon accreted from material similar to the Earth, as clearly shown by oxygen isotopes (Clayton and Mayeda, 1975; Hartmann *et al.*, 1986; Halliday, 2000). It is required that the Moon initially was in a completely or partially molten state (Canup and Agnor, 2000). Tidal interaction between the Earth and the Moon led to a quite stable orbital configuration of the satellite having a spin period equal to its orbital period, but slowing down the Earth with the Moon receding from the Earth (opposite to the Mars – Phobos situation, where the satellite is believed to move towards the main body (Yoder, 1995)). Due to the synchronous rotation of the Moon only half of the lunar surface is visible from Earth (near–side). The Moon, lacking an atmosphere, allows us even with the naked eye to identify bright and dark regions: the Face of the Moon. The near–side of the Moon is characterized by extensive darkish almost flat lava plains (Maria), mountain chains and brighter heavily cratered highland plateaus (Fig. 4.2).

The brighter plateaus are of anorthositic composition, and the primordial crust originated in the very beginning of the lunar geological history about 4.6 to 4.5 Ga ago (Halliday, 2000). This composition suggests fractional crystallization and differentiation from a global magma ocean (Taylor, 1982). The second stage of the evolution of lunar highland crust was its modification during a period from 4.4 to 3.9 Ga through the crystallization of mafic and ultramafic plutonic rocks (Shearer and Papike, 1999; James, 1980). Because the Moon, as all terrestrial planets, experienced a period of heavy bombardment (until 3.9 Ga ago), all of these early periods of magmatism, crust formation, and lunar mantle evolution are not preserved. The early upper lunar crust is perforated by impact craters of diverse sizes, covered by their polymict ejecta, and fractured and brecciated to depths of up to 20 km (megaregolith, Hartmann, 1973a). Mare basaltic magmatism followed the heavy bombardment period and basin formation, and occurred between 3.9 and 2 Ga ago. In small areas the gradual decay of volcanic activity even went on until 1 Ga ago, (e. g. Nyquist and Shih, 1992, and based on crater counts: Schaber (1973), or Hiesinger *et al.* (2002)).

Whereas impact cratering is a spatially random process, the maria are far from uniformly distributed. Images from the Moon's farside (Fig. 4.2) clearly show that more than 90% of the surface area of the lunar basaltic lava flows are located on the Earth–facing hemisphere,

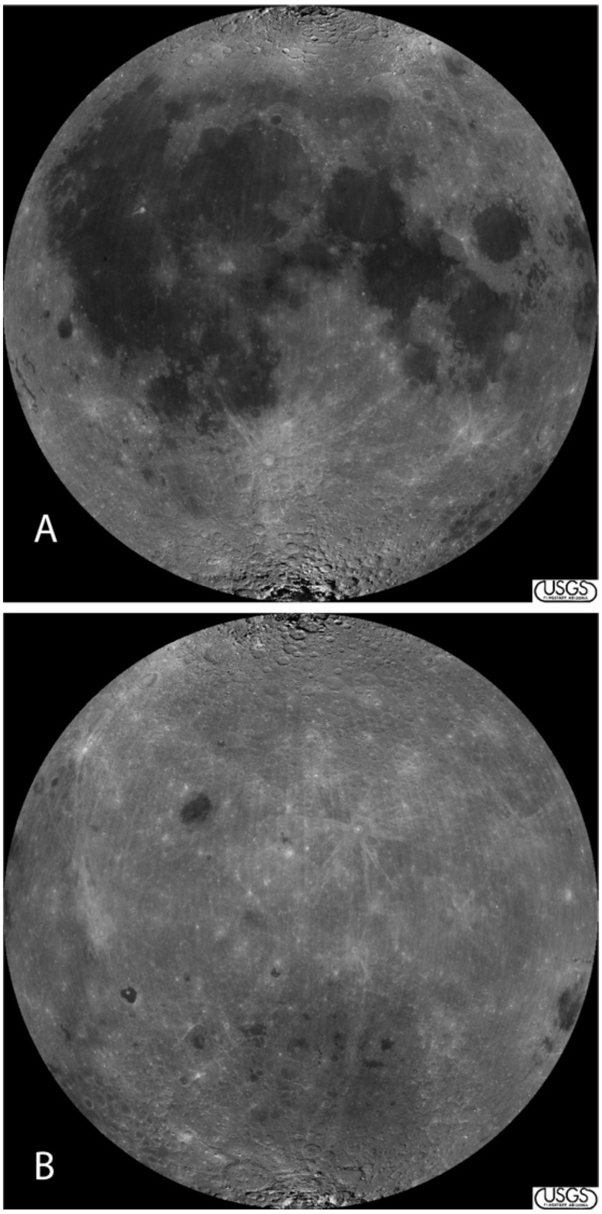

Figure 4.2.: Global Albedo Map of the Moon: These mosaics were processed by the U.S. Geological Survey, Flagstaff, Arizona, from images taken at a wavelength of 750 nm by Clementine (resolution: 5 km/pixel). In (A) the Earth–facing (near–side) of the Moon is shown, and in (B) the far–side.

and which is over 17 % of the total lunar surface (Head, 1975).

4.2. The Chronostratigraphy of the Moon

For planetary bodies, including the Moon, the stratigraphic system is based on photogeological mapping. In the case of the Moon, the lunar mapping and stratigraphic analysis was first derived from Earth–based telescopic photography and later updated from Lunar Orbiter and Apollo imagery. The boundaries of the lunar epochs are characterized by the formation of several large impact basins and a few younger craters. This was established by Shoemaker and Hackman (1962), using principles outlined by Gilbert (1893) and subsequently desribed comprehensively by Wilhelms (1987). The time–stratigraphic units are named (Fig. 4.3):

- Copernican System (the youngest)
- Erastosthenian System
- Upper Imbrian Series
- Lower Imbrian Series (nowadays, the Upper and Lower Imbrian Series are combined to the Imbrian System)
- Nectarian System
- Pre-Nectarian System (the oldest)

When investigating planetary geology and their sequences, local and regional interpretation are based on the principle of superposition, i.e. younger units overlie, cut, or overlap older ones. It is obvious that older units could accumulate more impact craters than younger surfaces, a principle that is used to understand relative surface ages (Öpik, 1960). As a standard method, crater frequencies are used to understand sequential processes when superposition relationships are lacking (e. g. Öpik, 1960; Shoemaker *et al.*, 1962; Baldwin, 1963, 1964; Hartmann, 1965, 1966; Soderblom, 1970; Neukum *et al.*, 1975; Neukum, 1983). The lunar stratigraphic system has been related to crater size–frequency schemes, so that geological units could be classified globally. In this

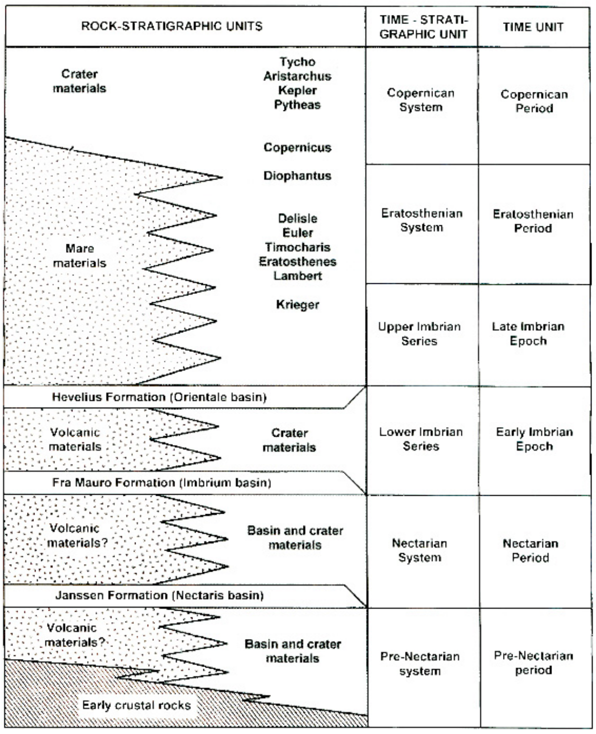

Figure 4.3.: The Lunar Stratigraphic Units (Wilhelms, 1987).

sense, craters are treated as a fossil Earth analogue for remote dating of planetary surfaces (McGill, 1977).

The first attempts to count craters on the Moon were based on telescopic photos. The diameter distribution for crater diameters larger than 1-2 km (see review by Hartmann, 2004) was recognized to be fitted in double logarithmic scale by a linear approach similar to the asteroid diameter distribution power laws:

$$\log N \;=\; k\,\log D^b, \tag{4.1}$$

where N can be understood as cumulative number of craters, D is the diameter and $b \sim -2$ for lunar craters. Nevertheless, Hartmann has consistently used log–incremental plots where N is the incremental number of craters in diameter bins of constant $\delta log D$. Mathematically, plotting cumulative or incremantal crater frequencies of craters larger than D result in identical slope steepnesses. A more comprehensive study gives a least–squares fit slope of -1.8 for lunar craters in this branch (Basaltic Volcanism Study Project, Hartmann *et al.*, 1981). Traditionally, this branch (i.e. larger than 1–2 km) is called *primary*, connoting that the craters originated from cosmic projectiles impacting with high speed.

To improve the method of determining surface ages by crater frequency measurements, and to better understand crater formation, the lunar craters have been investigated in detail by their morphology and size–frequency distributions. Lunar maria are smooth, homogeneous, and with clearly defined surface units, on which for most crater–size ranges representative distributions can be measured (i.e. no saturation limit has been reached). Crater counts on lunar maria are used to derive analytical descriptions of the *crater production function*. Partly based on astronomical observations, Shoemaker (1977); Hartmann and Wood (1971); Baldwin (1971); Hartmann *et al.* (1981); Chapman and Haefner (1967) favoured power–law dependences to delineate the crater distributions. For the smaller–size range, from about 1 km down to about 250 m (visible in lunar maria), $b = -3.82$ is a representative slope for this branch (Hartmann *et al.*, 1981). This second branch was suspected to be due to secondary craters produced by ejecta from lunar primary craters (Shoemaker, 1965).

One of the best power–law approaches advocated by W. K. Hartmann, describes the crater production function by a piece–wise three–segment power law:

$$\begin{aligned}
\log N &= -2.616 - 3.82\,\log D, \\
\text{for} &\quad D < 1.41\,\text{km} \\
\log N &= -2.920 - 1.80\,\log D, \\
\text{for} &\quad 1.41\,\text{km} < \text{D} < 64\,\text{km} \\
\log N &= -2.198 - 2.20\,\log D, \\
\text{for} &\quad D > 64\,\text{km}
\end{aligned} \tag{4.2}$$

This crater production function is a result of averaging individual crater counts in different mare areas.

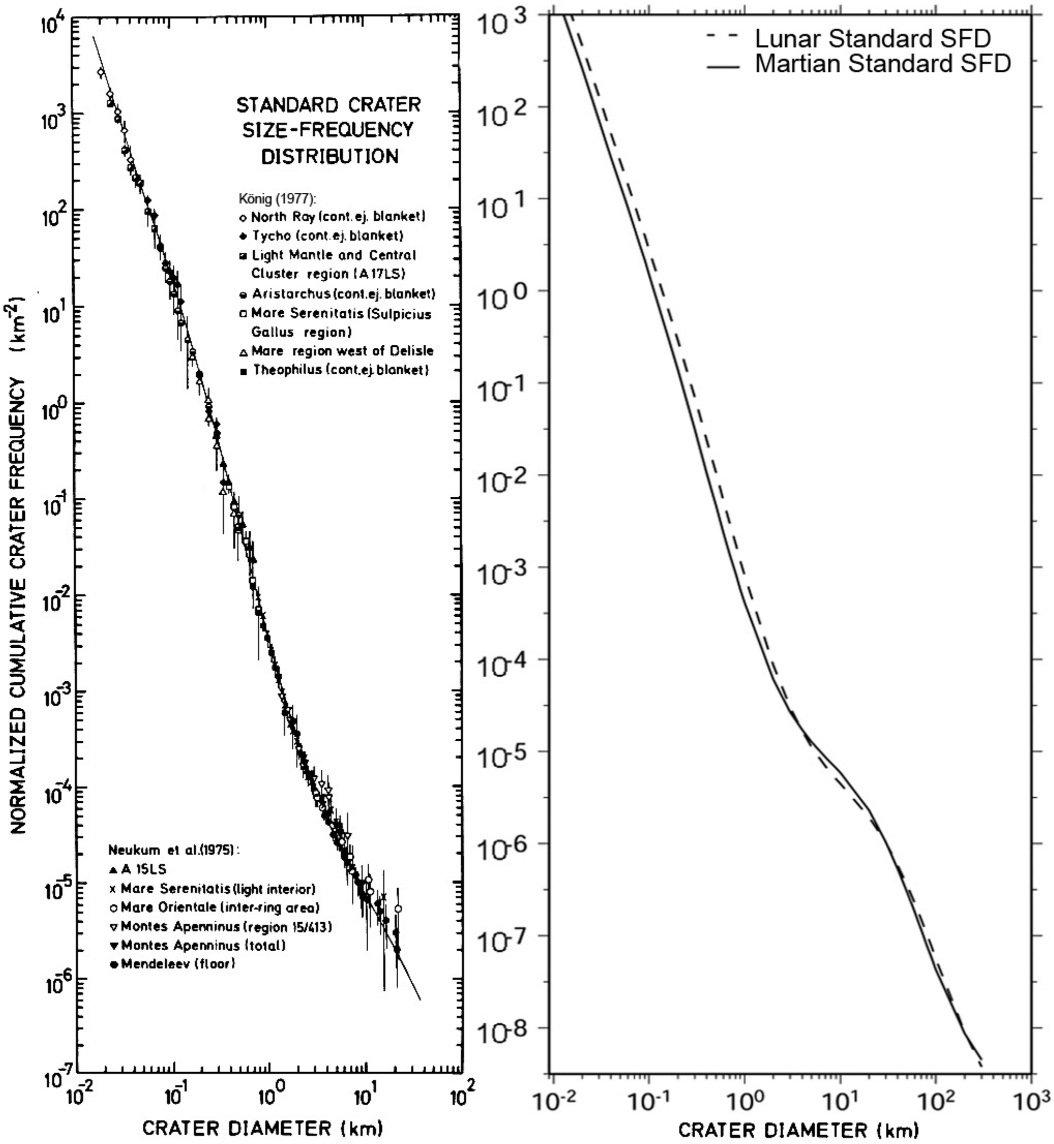

Figure 4.4.: The lunar crater production function from Neukum *et al.* (1975) and refined by Ivanov *et al.* (1999, 2001). The polynomial expression of eleventh order is given in equation 4.3.

Neukum *et al.* (1975, followed up by Neukum and König (1976); König (1977)) undertook a detailed analysis of the distribution measuring lunar crater populations on geologically homogeneous areas of various age, and over a wide diameter range. They did not follow the concept of multiple power–law segments and fitted the following polynomial function:

$$\log N = \sum_{j=0}^{11} a_j \, [\log D]^j, \qquad (4.3)$$

which is somewhat s–shaped (Fig. 4.4). This crater production function is applicable to craters on the Moon, on other planets such as Mars with appropriate scaling considerations, and on asteroids (Neukum, 1983), which will be discussed later.

Neukum *et al.* (1975); Neukum (1983); Neukum and Ivanov (1994) were able to show that the shape of the crater size–frequency distribution is stable and approximatly invariant through time. Neukum and Ivanov (1994) proved the steep branch among sub-kilometer asteroidal craters as well as in the asteroid belt, and in the near-Earth orbit population (Werner *et al.*, 2002). Henceforth, they disproved the Shoemaker-era idea, that the steep branch on the Moon (or Mars) is associated with secondary ejecta from lunar (and Martian) primary craters. Hartmann (1999b, and others) pointed out that the steep branch found in the asteroid belt is presumably due to secondary "ejecta" from craters on asteroids, except that the fragments do not fall back onto the target asteroids but rather float in the belt and hit other asteroids, i.e. a collisionally evolved projectile distribution (e.g. Hartmann and Hartmann, 1968; Wetherill, 1967, 1979).

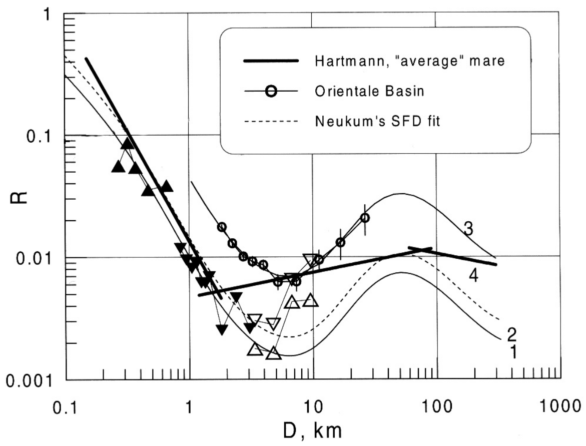

Figure 4.5.: Comparison between the two standard crater production function derived by Hartmann and Neukum in the R–representation. (filled triangles: crater counts at the Apollo 17 landing site by Neukum (1983) open triangles: counts by Hartmann *et al.* (1981)), 1, 2, 3: crater production function by Neukum, 4 crater production function by Hartmann.

Over the past few years, the lunar crater production function has been slightly refined (Ivanov *et al.*, 1999, 2001) by remeasuring the larger–crater part in the Orientale basin, and discussed in comparison with the Hartmann approach (Neukum *et al.*, 2001). While Hartmann's crater production function is based on averaged measurements in lunar maria, Neukum's crater production function is based on a number of measurements covering the full crater–size range. Comparing both approaches in R–plot form (differential size frequencies divided by D^{-3}) they fit observational data quite well. A maximum discrepancy to Hartmann's approach of a factor of 3 is observed in the diameter bins around $D = 6$ km (Neukum *et al.*, 2001). As demonstrated in Figure 4.5, the crater production function by Neukum fits observations slightly better.

Figure 4.6.: The Apollo and Luna landing–sites.

Ground–truth data in terms of absolute ages is, besides Earth, available only for the Earth's moon, and was gained when the first rock samples from the Moon were returned to Earth (Fig. 4.6). These were collected by astronauts at six Apollo landing sites. In addition, robotic sample returns came from Luna landings. Sampling locations, regional geology, and the abso-

Lunar Chronostratigraphy

System	Boundary structure	Radiometric Age [Ga]	Crater Frequency N(1) [km^{-2}]	Absolute Crater Retention Age [Ga]*
Copernican				
	Crater Copernicus	0.85	1.3 10^{-3}	1.5
Erastosthenian				
	Crater Erastosthenes		3.0 10^{-3}	3.2
Upper Imbrian				
	Orientale basin			3.7
Lower Imbrian				
	Imbrium basin	3.9	3.5 10^{-2}	3.9
Nectarian				
	Nectaris basin	4.1	1.2 10^{-1}	4.1
Pre-Nectarian				
	Highlands	4.4	3.6 10^{-1}	4.3

* Ga, Giga anni (Latin: billion of years)

Table 4.1.: Epochs, cumulative crater frequencies N(1) (N: number of craters equal to and larger than 1 km in diameter per square kilometer), and absolute ages: The link to absolute ages are based on rock ages determined for the returned samples collected at the Apollo and Luna landing sites, see Fig. 4.6 (from Neukum, 1983).

lute ages of lunar rocks are known and therefore the absolute age of geological units. The first absolute ages could be more or less confidently related to crater size frequency measurements. Approximately 20 lunar meteorites generally support the distinction between highland and mare terrain, but cannot be ascribed to specific surface units (Grossman, 2000). Stöffler and Ryder (2001) provide an extensive review of all absolute rock ages and their reliability. They pointed out that the geologic and stratigraphic interpretation of isotope ages of lunar rock is not always straightforward because none of the rock samples was collected from bedrock units.

Cumulative crater size–frequency distributions measured for major rock–stratigraphic and time–stratigraphic units of the Moon's history are listed in Fig. 4.3.

Combining these cumulative crater frequencies as a function of lunar surface ages, a calibration curve allows for deriving a cratering rate in the Earth–Moon system as a function of time. This *cratering chronology model* is given here as expressed analytically by Neukum (1983) for crater size–frequency distributions, and related surface ages (Table 4.1):

$$N(\geq 1\text{km}) = 5.44 \cdot 10^{-14}[\exp(6.93\text{T}) - 1] + 8.38 \cdot 10^{-4}T \quad (4.4)$$

where N is the number of craters equal to and larger than 1 km in diameter per square kilometer in an area and T is the crater accumulation time (crater retention age) in Ga (Giga anni (Latin: billion of years)). This function is illustrated in Figure 4.7. Many other chronology models for the lunar cratering rate and the absolute retention ages (see Neukum, 1983; Wilhelms, 1987), based on similar sets of ages, have been published. All curves have in common that the cratering rate during the last 3 Ga was relatively constant within a factor of 2. Before this time, the cratering projectile flux was rapidly, exponentially decaying in time. This early period, in which 95% of the lunar craters were formed, is referred to as the *late heavy bombardment.*

The flux difference between the first half billion years and the following 3 to 4 billion years is observed on the surface of those planets and moons that lack the obliteration effect of geologic activity. The discrepancy in crater frequencies between heavily cratered terrains and

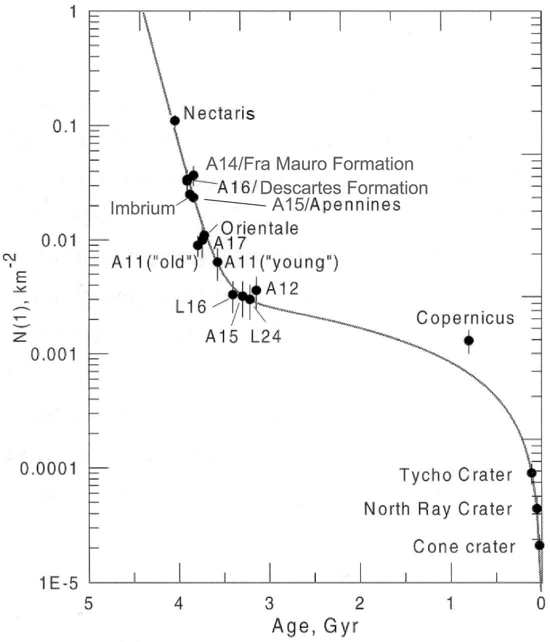

Figure 4.7.: The lunar chronology model with the referring ages and crater size frequencies of the landings sites (see also Fig. 4.6 and Table 4.1).

less cratered plains units appears to be a 3.9 Ga marker horizon throughout the inner solar system (Wetherill, 1975). It was believed, that this projectile flux might be the remnant of the planetary formation period and asteroids left over from this period (further discussion in Chapter 5.2).

Cratering rates, absolute surface ages, and a chronology model for the Moon allow us to establish an absolute lunar stratigraphy and to provide a standard reference curve for stratigraphic time that is applicable to other planetary bodies. This will be discussed in the following chapters with special focus on Mars.